



Communication

Phosphodiesterases 3 and 4 Differentially Regulate the Funny Current, I_f , in Mouse Sinoatrial Node Myocytes

Joshua R. St. Clair¹, Eric D. Larson¹ , Emily J. Sharpe¹, Zhandi Liao¹ and Catherine Proenza^{1,2,*} 

¹ Department of Physiology and Biophysics, University of Colorado School of Medicine, Aurora, CO 80045, USA; joshua.stclair@ucdenver.edu (J.R.S.); eric.larson@ucdenver.edu (E.D.L.); emily.sharpe@ucdenver.edu (E.J.S.); zdliao@ucdavis.edu (Z.L.)

² Department of Medicine, Division of Cardiology, University of Colorado School of Medicine, Aurora, CO 80045, USA

* Correspondence: catherine.proenza@ucdenver.edu; Tel.: +1-303-724-2522

Received: 30 June 2017; Accepted: 19 July 2017; Published: 1 August 2017

Abstract: Cardiac pacemaking, at rest and during the sympathetic fight-or-flight response, depends on cAMP (3',5'-cyclic adenosine monophosphate) signaling in sinoatrial node myocytes (SAMs). The cardiac “funny current” (I_f) is among the cAMP-sensitive effectors that drive pacemaking in SAMs. I_f is produced by hyperpolarization-activated, cyclic nucleotide-sensitive (HCN) channels. Voltage-dependent gating of HCN channels is potentiated by cAMP, which acts either by binding directly to the channels or by activating the cAMP-dependent protein kinase (PKA), which phosphorylates them. PKA activity is required for signaling between β adrenergic receptors (β ARs) and HCN channels in SAMs but the mechanism that constrains cAMP signaling to a PKA-dependent pathway is unknown. Phosphodiesterases (PDEs) hydrolyze cAMP and form cAMP signaling domains in other types of cardiomyocytes. Here we examine the role of PDEs in regulation of I_f in SAMs. I_f was recorded in whole-cell voltage-clamp experiments from acutely-isolated mouse SAMs in the absence or presence of PDE and PKA inhibitors, and before and after β AR stimulation. General PDE inhibition caused a PKA-independent depolarizing shift in the midpoint activation voltage ($V_{1/2}$) of I_f at rest and removed the requirement for PKA in β AR-to-HCN signaling. PDE4 inhibition produced a similar PKA-independent depolarizing shift in the $V_{1/2}$ of I_f at rest, but did not remove the requirement for PKA in β AR-to-HCN signaling. PDE3 inhibition produced PKA-dependent changes in I_f both at rest and in response to β AR stimulation. Our results suggest that PDE3 and PDE4 isoforms create distinct cAMP signaling domains that differentially constrain access of cAMP to HCN channels and establish the requirement for PKA in signaling between β ARs and HCN channels in SAMs.

Keywords: sinoatrial node; HCN channel; funny current (I_f); cardiac pacemaking; cardiomyocyte; cell compartmentalization; phosphodiesterases; cyclic AMP (cAMP); ion channel; patch clamp

1. Introduction

Cardiac pacemaking, at rest and during the sympathetic fight-or-flight response, depends on cAMP signaling in sinoatrial node myocytes (SAMs). SAMs are highly-specialized cells that drive pacemaking by firing spontaneous action potentials (APs). Spontaneous APs in SAMs result from a spontaneous depolarization during diastole that drives the membrane potential to its threshold to initiate the subsequent AP. The diastolic depolarization in SAMs arises as a function of the coordinated activity of a unique complement of ion channels that work in concert with intracellular Ca^{2+}

signaling [1–4]. 3',5'-cyclic adenosine monophosphate (cAMP) is a critical regulator of pacemaking in SAMs. The resting cytoplasmic concentration of cAMP is thought to be higher in SAMs than in other cardiac myocytes [5] and sympathetic nervous system stimulation increases heart rate by activating β adrenergic receptors (β ARs) and further increasing cAMP in SAMs.

The “funny current” (I_f) is a hallmark of SAMs and is among the many cAMP-sensitive effectors that contribute to spontaneous pacemaker activity in SAMs. I_f is produced by hyperpolarization-activated, cyclic nucleotide-sensitive (HCN) ion channels. HCN4 is the predominant HCN channel isoform in the sinoatrial node of all mammals; it is expressed at high levels in SAMs and is used as a marker of the sinoatrial node [6–9]. I_f is activated by membrane hyperpolarization and is a mixed cationic conductance with a reversal potential of approximately -30 mV in physiological solutions [10,11]. Thus, I_f is inward at diastolic potentials, and it is thought to contribute to the diastolic depolarization phase of the sinoatrial AP. In accordance with a critical role for I_f in pacemaking, mutations in HCN4 channels cause sinoatrial node dysfunction in human patients and animal models [12–14] and HCN channel blockers decrease the heart rate [15,16].

cAMP potentiates voltage-dependent gating of HCN4 channels either by binding directly to a conserved cyclic nucleotide binding domain in the proximal C-terminus [17,18] or by protein kinase A (PKA)-mediated phosphorylation of the distal C-terminus [11]. In either case, cAMP causes a depolarizing shift in the midpoint activation voltage ($V_{1/2}$). We previously showed that PKA activity is necessary for cAMP-dependent signaling between β ARs and HCN channels in SAMs; inhibition of PKA with an inhibitory peptide, PKI, significantly reduced the shift in $V_{1/2}$ produced by β AR stimulation [11]. However, we have also shown that HCN channels in SAMs can be activated by cAMP even in the absence of PKA activity [19], presumably by binding directly to the channels. Thus, the requirement for PKA in β AR-to-HCN4 channel signaling in SAMs could arise as a function of compartmentalization or restricted diffusion of cAMP [19].

Although cAMP is a small, soluble molecule, it does not behave as a freely-diffusing molecule in many types of cells [20–27]. cAMP concentration in cells is determined by a balance between production by adenylyl cyclases and degradation by cyclic nucleotide phosphodiesterases (PDEs). PDEs have been shown to form functional diffusion barriers in other types of cardiac myocytes [28–32]. PDEs are organized into 11 families, of which the PDE3 and PDE4 families are the most abundant in the mouse sinoatrial node [33]. Functional studies using subtype-specific inhibitors have shown that the PDE3 and PDE4 families regulate the beating rate of mouse right atrial preparations [34], as well as the AP firing rate and Ca^{2+} currents in isolated mouse SAMs [33]. PDE4 is specific for cAMP, although it has a relatively low affinity (2–8 μ M). In contrast, PDE3 can hydrolyze both cAMP and cGMP, but has a high affinity for cAMP (10–100 nM). Hydrolysis of cAMP by PDE3 is inhibited by cGMP due to a \sim 10-fold slower maximum reaction rate for cGMP [35,36].

In this study we tested the hypothesis that PDEs contribute to regulation of I_f in SAMs by creating functional cAMP signaling domains. Indeed, we found that the PDE3 and PDE4 isoforms play distinct roles in regulation of I_f , such that PDE4s control access of cAMP to HCN channels at rest, while PDE3s interact functionally with PKA to constrain signaling between β ARs and HCN channels in SAMs.

2. Materials and Methods

2.1. Ethical Approval

This study was carried out in accordance with the US Animal Welfare Act and the National Research Council's *Guide for the Care and Use of Laboratory Animals* and was conducted according to a protocol that was approved by the University of Colorado-Anschutz Medical Campus Institutional Animal Care and Use Committee (protocol number 84814(06)1E). Six- to eight-week old male C57BL/6J mice were obtained from Jackson Laboratories (Bar Harbor, ME, USA; Cat. #000664). Animals were anesthetized by isoflurane inhalation and euthanized under anesthesia by cervical dislocation.

2.2. Sinoatrial Myocyte Isolation

Sinoatrial myocytes were isolated as we have previously described [11,19,37–42]. Briefly, hearts were removed into heparinized (10 U/mL) Tyrodes solution at 35 °C (in mM: 140 NaCl, 5.4 KCl, 1.2 KH₂PO₄, 1.8 MgCl₂, 1 CaCl₂, 5 HEPES, and 5.55 glucose, with pH adjusted to 7.4 with NaOH). The sinoatrial node, as defined by the borders of the crista terminalis, the interatrial septum, and the inferior and superior vena cavae, was excised and digested in an enzyme cocktail consisting of collagenase type II (Worthington Biochemical, NJ, USA), protease type XIV (Sigma Aldrich, St. Louis, MO, USA), and elastase (Worthington Biochemical, Lakewood, NJ, USA) for 25–30 min at 35 °C in a modified Tyrodes solution (in mM: 140 NaCl, 5.4 KCl, 1.2 KH₂PO₄, 5 HEPES, 18.5 glucose, 0.066 CaCl₂, 50 taurine, and 1 mg/mL BSA; pH adjusted to 6.9 with NaOH). Tissue was transferred to a modified KB solution (in mM: 100 potassium glutamate, 10 potassium aspartate, 25 KCl, 10 KH₂PO₄, 2 MgSO₄, 20 taurine, 5 creatine, 0.5 EGTA, 20 glucose, 5 HEPES, and 0.1% BSA; pH adjusted to 7.2 with KOH) at 35 °C, and cells were dissociated by trituration with a fire-polished glass pipet for ~10 min. Ca²⁺ was gradually reintroduced, and dissociated cells were maintained at room temperature for up to 8 h prior to electrophysiological recordings.

2.3. Sinoatrial Myocyte Electrophysiology

For electrophysiology, an aliquot of the sinoatrial node myocyte suspension was transferred to a glass-bottomed recording chamber on the stage of an inverted microscope. Individual SAMs were identified by spontaneous contractions, characteristic morphology [11,19,37–42], capacitance <45 pS, and the presence of I_f. Borosilicate glass pipettes had resistances of 1–3 MΩ when filled with an intracellular solution containing (in mM): 135 potassium aspartate, 6.6 sodium phosphocreatine, 1 MgCl₂, 1 CaCl₂, 10 HEPES, 10 EGTA, 4 Mg-ATP; pH adjusted to 7.2 with KOH. SAMs were constantly perfused (1–2 mL/min) with Tyrodes solution containing 1 mM BaCl₂ to block K⁺ currents. A 1 mM stock solution of isoproterenol hydrochloride (ISO; Calbiochem/EMD Millipore, Billerica, MA, USA) in 1 mM ascorbic acid was stored as frozen aliquots, which were thawed on the day of experimentation and added to the perfusing Tyrodes solution to a final concentration of 1 μM as indicated.

Whole cell voltage clamp recordings were performed >2 min after achieving the whole cell recording configuration, to allow for intracellular perfusion with the pipette solution. To determine the voltage dependence of I_f, families of currents were elicited by 3 s hyperpolarizing voltage steps ranging from –60 mV up to –170 mV in 10 mV increments from a holding potential of –35 mV, as previously described [11,19,37–42]. Although steady state activation of I_f is not attained within 3 s for more depolarized potentials owing to the very slow kinetics of activation of I_f, the protocol is an experimentally-feasible means to approximate and compare the voltage-dependence of activation of I_f in the presence of different inhibitors (see [11]). Conductance (G) was calculated from the inward currents as:

$$G = I / (V_m - V_r) \quad (1)$$

where *I* is the time-dependent component of I_f, *V_m* is the applied membrane voltage (corrected for a +14 mV junction potential error, calculated using JPCalc [43]), and *V_r* is the reversal potential for I_f under these experimental conditions (–30 mV; [10,11]). Conductances were plotted as a function of voltage, and isochronal midpoint activation voltages (*V*_{1/2}) were determined for each cell by fitting with a Boltzmann function:

$$f(V) = V_{\min} + \frac{V_{\max} - V_{\min}}{1 + e^{\frac{z_d F}{RT}(V - V_{1/2})}} \quad (2)$$

where *V_{min}* and *V_{max}* are the voltages corresponding to the minimum and maximum currents, *Z_d* is the charge valence, *R* is the gas constant, *T* is temperature, and *F* is the Faraday constant. The conductance-voltage relationship was determined for each individual cell included in the study and all individual GV relationships reached saturation. Averaged GV relationships are extrapolated to –170 for all conditions to facilitate comparisons. All experiments were conducted at room temperature in order to

access the full range of activation midpoints for I_f (approximately -110 to -130 mV). Three cells were considered outliers and were excluded from the datasets because their midpoint activation voltages were greater than two standard deviations from the mean.

The isoproterenol- (ISO-) dependent shift in voltage dependence ($\Delta V_{1/2}$ -ISO) was determined from paired recordings in individual cells before and after wash-on of $1 \mu\text{M}$ ISO in the absence or presence of PDE inhibitors. Current elicited by 1 s test pulses to -120 mV every 5 – 10 s was monitored during the ISO wash-on. The second GV protocol was begun when the increased current due to the ISO-dependent shift in $V_{1/2}$ reached steady state (within 1 – 2 min). PDE inhibitors were present in the extracellular solution as follows: total PDE inhibition with $100 \mu\text{M}$ 3-isobutyl-1-methylxanthine (IBMX; Tocris Bioscience, Bristol, UK), PDE4 inhibition with $10 \mu\text{M}$ rolipram (roli; Tocris Bioscience) or PDE3 inhibition with 10 or $50 \mu\text{M}$ milrinone (milr; Tocris Bioscience). The PKA inhibitory peptide 6-22 amide (PKI; Tocris Bioscience) was added to the intracellular (patch pipette) solution as noted at a final concentration of $10 \mu\text{M}$. The adenylyl cyclase inhibitor MDL-12,330A (MDL) was applied at a final concentration of $10 \mu\text{M}$ in the bath solution.

2.4. Statistical Analysis

Data are presented as mean \pm SEM. Statistical significance was evaluated by paired or unpaired two-tailed t tests or one-way ANOVAs with post-hoc tests as indicated. A p value of <0.05 was considered to be statistically significant.

3. Results

3.1. Phosphodiesterases Restrict Access of cAMP to HCN Channels at Rest

To evaluate the overall effects of PDEs on I_f in mouse SAMs, we applied the general, non-subtype-selective PDE inhibitor, 3-isobutyl-1-methylxanthine (IBMX; $100 \mu\text{M}$ in the extracellular solution) to acutely isolated SAMs in whole-cell voltage-clamp experiments. We found that IBMX shifted the midpoint activation voltage ($V_{1/2}$) of I_f by ~ 15 mV to more depolarized potentials (Figure 1A,C; Table 1), consistent with an increase in cAMP concentration in the vicinity of the HCN channels. Thus PDEs limit access of basal cAMP to HCN channels at rest.

Since we previously found that PKA activity is required for the cAMP-dependent activation of I_f by β ARs in SAMs [11], we next asked whether PKA is also required for the cAMP liberated by IBMX to activate I_f . To this end, we evaluated the effects of IBMX on I_f in SAMs in which PKA was inhibited by the pseudosubstrate inhibitory peptide, PKI 6-22 amide (PKI; $10 \mu\text{M}$ in the patch pipette). We found that IBMX had essentially identical effects in the presence or absence of PKI; the $V_{1/2}$ of I_f did not differ in IBMX versus IBMX plus PKI (Figure 1C). Thus, in contrast to the cAMP generated upon β AR stimulation, the basal cAMP released upon PDE inhibition can activate HCN channels in SAMs independent of PKA activity.

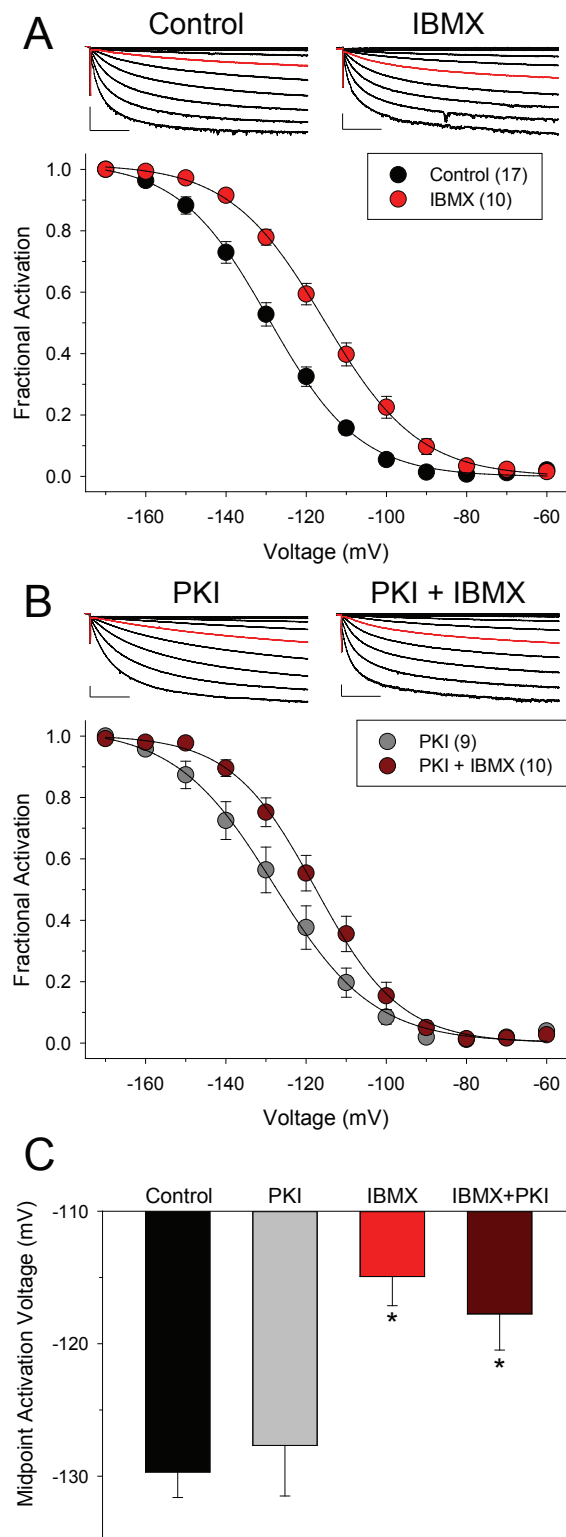


Figure 1. General PDE inhibition activates I_f in SAMs at rest via a PKA-independent mechanism. (A,B) Average (\pm SEM) normalized conductance-voltage plots for I_f in control (black), IBMX (100 μ M in extracellular solution; red), PKI (10 μ M in patch pipette; grey), or IBMX plus PKI (dark red). Numbers in parentheses in the legends indicate the number of cells in each dataset. Insets show representative I_f current families. Red traces show currents elicited by voltage steps to -120 mV to illustrate shifts in voltage dependence. Scale bars, 200 pA, 500 ms; and (C) average (\pm SEM) $V_{1/2}$ for I_f for the indicated conditions. Asterisks indicate $p < 0.05$ versus control; one-way ANOVA with Holm-Sidak post-test.

Table 1. Midpoint activation voltages for I_f in mouse sinoatrial myocytes. $V_{1/2}$ values for I_f were determined in the absence or presence of PDE inhibitors (IBMX 100 μ M, rolipram 10 μ M, milrinone 10 μ M, or 50 μ M as indicated) in the extracellular solution with and without the PKA inhibitory peptide, PKI (10 μ M) in the pipette solution. For each cell, $V_{1/2}$ values were determined before or after wash-on of 1 μ M isoproterenol in the extracellular solution; $\Delta V_{1/2(ISO)}$ is the average ISO-induced shift in $V_{1/2}$. Data for cAMP (1 mM in the patch pipette) and MDL-12,330A (10 μ M in the extracellular solution) are provided for comparison from [13].

Treatment	$V_{1/2}$ before ISO (mV)	$V_{1/2}$ after ISO (mV)	$\Delta V_{1/2}$ -ISO (mV)	n	p Value Control vs. ISO (Paired t-Test)
CONTROL	-129.7 ± 1.9	-119.6 ± 1.5	10.1 ± 1.2	17	0.000000237
+PKI	-127.7 ± 3.8	-123.6 ± 3.5	4.1 ± 0.7	9	0.00188
IBMX	-114.9 ± 2.2	-110.1 ± 2.8	4.8 ± 1.9	10	0.0328
+PKI	-117.7 ± 2.7	-110.6 ± 2.7	7.1 ± 1.1	10	0.000128
ROLIPRAM	-117.4 ± 1.6	-113.4 ± 2.2	4.0 ± 1.1	9	0.00712
+PKI	-118.9 ± 3.0	-118.8 ± 2.8	0.1 ± 1.9	7	0.967
MILRINONE (10 μ M)	-124.0 ± 4.3	-121.1 ± 4.7	2.9 ± 1.7	8	0.123
+PKI	-119.3 ± 4.7	-112.5 ± 4.8	6.8 ± 2.4	10	0.0206
MILRINONE (50 μ M)	-124.1 ± 1.9	-122.2 ± 2.0	1.8 ± 1.0	10	0.104
+PKI	-116.8 ± 1.3	-110.9 ± 1.8	5.9 ± 1.2	11	0.000648
MDL-12,330A	-131.1 ± 1.9	-132.0 ± 2.2	-0.9 ± 1.1	7	0.469
1 mM cAMP	-112.0 ± 1.6	-	-	10	-
3 mM cAMP	-114.1 ± 1.9	-	-	7	-

3.2. Different Effects of PDE4 and PDE3 on I_f under Basal Conditions

PDE4 activity is thought to regulate sinoatrial node pacemaker activity in a number of species, based on experiments using rolipram, a PDE4 family inhibitor [33,34,44,45]. To determine the role of PDE4 in basal regulation of I_f in mouse SAMs, we evaluated the effects of rolipram (10 μ M in the bath solution) on the $V_{1/2}$ of I_f . We found that rolipram caused a significant depolarizing shift in $V_{1/2}$ which was indistinguishable from the shift produced by IBMX (Figure 2A,C; Table 1). As in the case of IBMX, the rolipram-liberated cAMP did not require PKA activity in order to activate HCN channels, since the $V_{1/2}$ values did not differ in rolipram alone compared to rolipram plus PKI (Figure 2C; Table 1).

The PDE3 family is also thought to affect sinoatrial node function; inhibition of PDE3 increases basal pacemaker activity in isolated SAMs and atrial preparations from mice [33,34]. In contrast to IBMX or rolipram, we found that the PDE3 family inhibitor, milrinone (10 or 50 μ M) produced only a modest, statistically insignificant, depolarizing shift in the $V_{1/2}$ of I_f in SAMs when applied by itself (Figure 3A,C; Table 1). However, when milrinone was applied in the presence of PKI, it produced a significant depolarizing shift in $V_{1/2}$ of I_f , which was similar in magnitude to the shifts produced by IBMX or rolipram (Figure 3; Table 1).

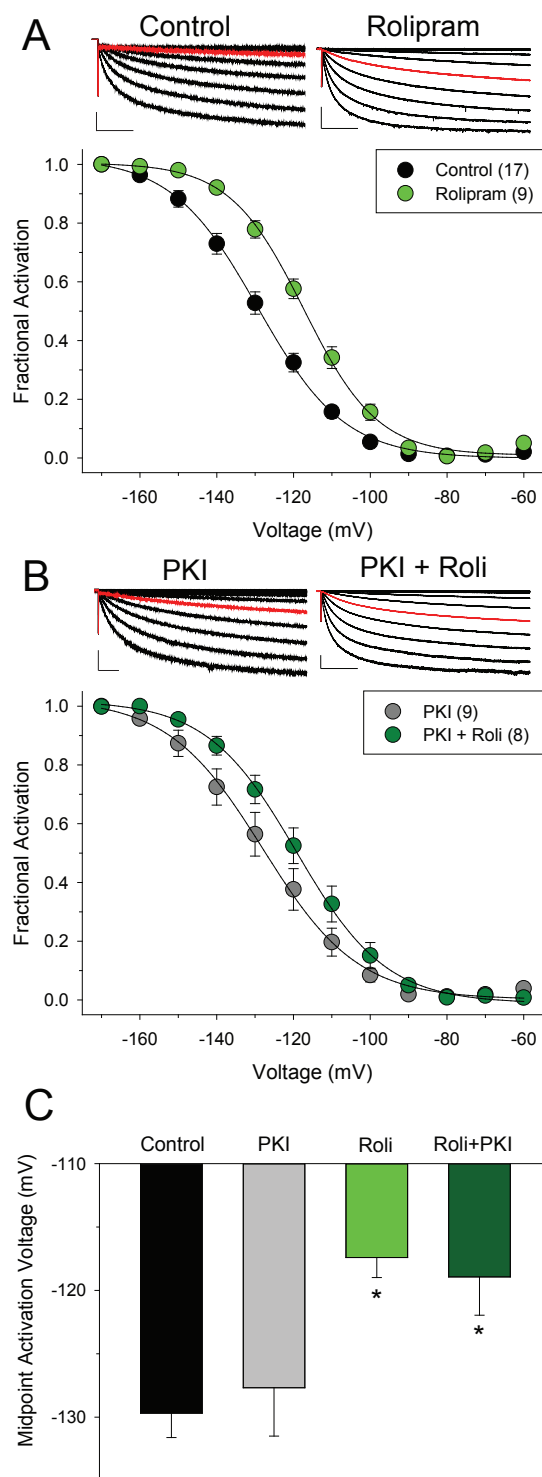


Figure 2. PDE4 inhibition activates I_f in SAMs at rest via a PKA-independent mechanism. **(A,B)** Average (\pm SEM) normalized conductance-voltage plots for I_f in control (black), rolipram (10 μ M in the extracellular solution; green), PKI (10 μ M in the patch pipette; grey), or PKI plus rolipram (dark green). Numbers in parentheses in the legends indicate the number of cells in each dataset. *Insets* show representative I_f current families. Red traces elicited by voltage steps to -120 mV illustrate shifts in the voltage dependence. Scale bars, 100 pA, 500 ms for control, 500 pA, 500 ms for PKI; and **(C)** shows the average (\pm SEM) $V_{1/2}$ for I_f for indicated conditions. *Asterisks* indicate $p < 0.05$ versus control; one-way ANOVA with Holm-Sidak post-test.

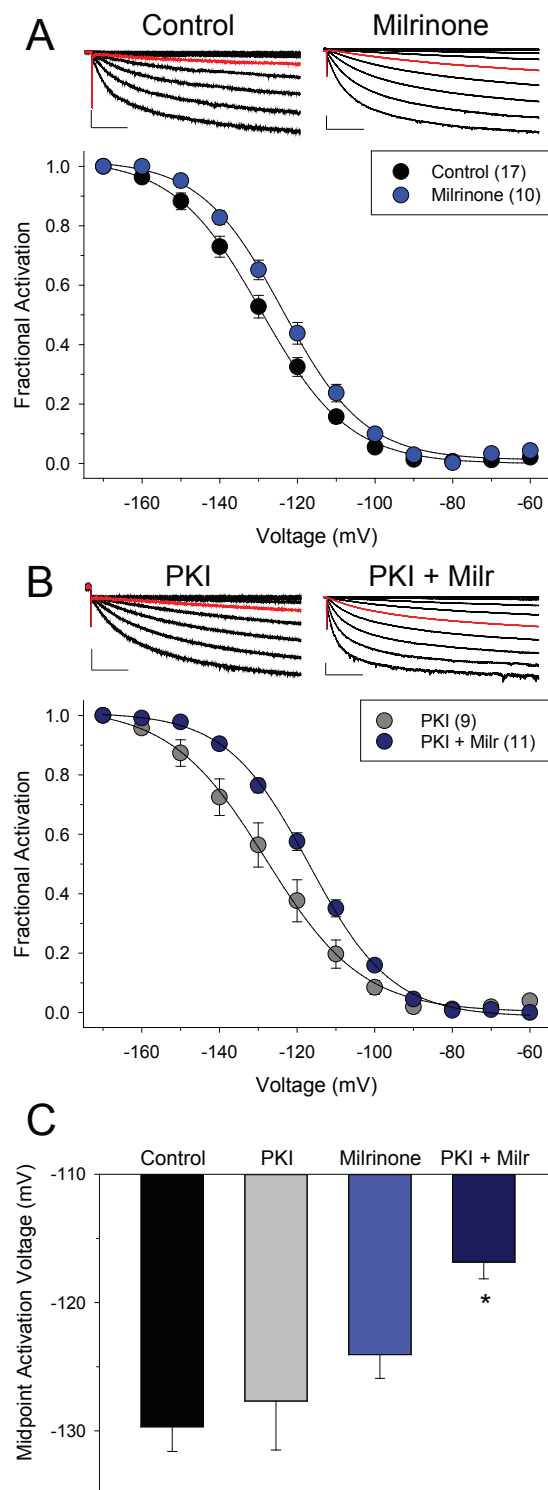


Figure 3. Effects of PDE3 inhibition on I_f at rest. (A,B) Average (\pm SEM) normalized conductance-voltage plots for I_f in control (black), milrinone (50 μ M in the extracellular solution; blue), PKI (10 μ M in the patch pipette; grey), or milrinone plus PKI (dark blue). Numbers in parentheses in the legends indicate the number of cells in each dataset. Insets show representative I_f current families. Red traces elicited by voltage steps to -120 mV illustrate shifts in the voltage dependence. Scale bars, 100 pA, 500 ms for control, 500 pA, 500 ms for PKI; and (C) shows the average (\pm SEM) $V_{1/2}$ for I_f for indicated conditions. Asterisk indicates $p < 0.05$ versus control; one-way ANOVA with Holm-Sidak post-test.

3.3. PDEs Establish the Requirement for PKA Activity in Signaling between β ARs and HCN Channels in SAMs

To evaluate the role of PDEs in establishing the requirement for PKA in β AR-to-HCN channel signaling in SAMs, we assayed the shift in $V_{1/2}$ in individual cells in response to the wash-on of the β AR agonist, isoproterenol ($\Delta V_{1/2}$ -ISO). $\Delta V_{1/2}$ -ISO shifts were determined in the absence or presence of PDE inhibitors and PKI. In control Tyrode's solution, the wash-on of ISO produced a ~10 mV depolarizing shift in the $V_{1/2}$ of I_f (Figure 4A). In the presence of PKI in the patch pipette (but the absence of any PDE inhibitors), ISO still produced a significant shift in $V_{1/2}$ in paired recordings from individual cells, but the magnitude of this shift was significantly reduced compared to control (Figure 4A; Table 1). In cells treated with IBMX, ISO produced a significant ~5 mV depolarizing shift in $V_{1/2}$, in addition to the ~15 mV shift already caused by IBMX (Figure 4B; Table 1). We attribute the reduced $\Delta V_{1/2}$ -ISO in IBMX versus control (Figure 4B versus Figure 4A) to a ceiling effect, because the absolute value of the $V_{1/2}$ in IBMX plus ISO (approximately -110 mV) did not differ from that produced by a saturating concentration of cAMP introduced via the patch pipette (approximately -112 mV; Table 1). Whereas PKI significantly decreased the $\Delta V_{1/2}$ -ISO under control conditions (Figure 4A), it did not reduce $\Delta V_{1/2}$ -ISO when PDEs were inhibited by IBMX (Figure 4B). Thus, PDEs contribute to the formation of the PKA-dependent signaling pathway between β ARs and HCN channels in SAMs, apparently by restricting the ability of β AR-stimulated cAMP to access the channels.

The contributions of the PDE4 and PDE3 families to the PKA-dependent β AR-to-HCN channel signaling pathway were evaluated using rolipram or milrinone. In cells treated with rolipram, ISO produced a significant depolarizing shift in the $V_{1/2}$ of I_f (Figure 4C; Table 1). As in the case of IBMX, this ISO-dependent shift was reduced in magnitude compared to the shift in control conditions, and again, the reduction is attributed to a ceiling effect because the $V_{1/2}$ for rolipram plus ISO did not differ from that of saturating cAMP (Table 1). However, in contrast to the situation of general PDE block with IBMX, block of PDE4s with rolipram did not relieve the requirement for PKA in β AR-to-HCN channel signaling in SAMs. In fact, PKI completely abolished the ability of ISO to shift the $V_{1/2}$ in the presence of rolipram ($p = 0.967$ versus a hypothetical mean shift of 0; Figure 4C; Table 1). Thus, PDE4 does not appear to contribute to the PKA dependent β AR-to-HCN signaling pathway.

While the ability of ISO to shift the $V_{1/2}$ was nearly eliminated by the PDE3 inhibitor milrinone when it was applied alone ($p = 0.104$ versus a hypothetical mean shift of 0; Figure 4D; Table 1), simultaneous inhibition of both PDE3 and PKA, with milrinone plus PKI, restored the ability of ISO to shift in $V_{1/2}$ of I_f (Figure 4D; Table 1) consistent with a role for PDE3 in the formation of the PKA dependent β AR-to-HCN signaling pathway and, again, indicative of an interaction between PKA and PDE3 in the regulation of I_f in SAMs.

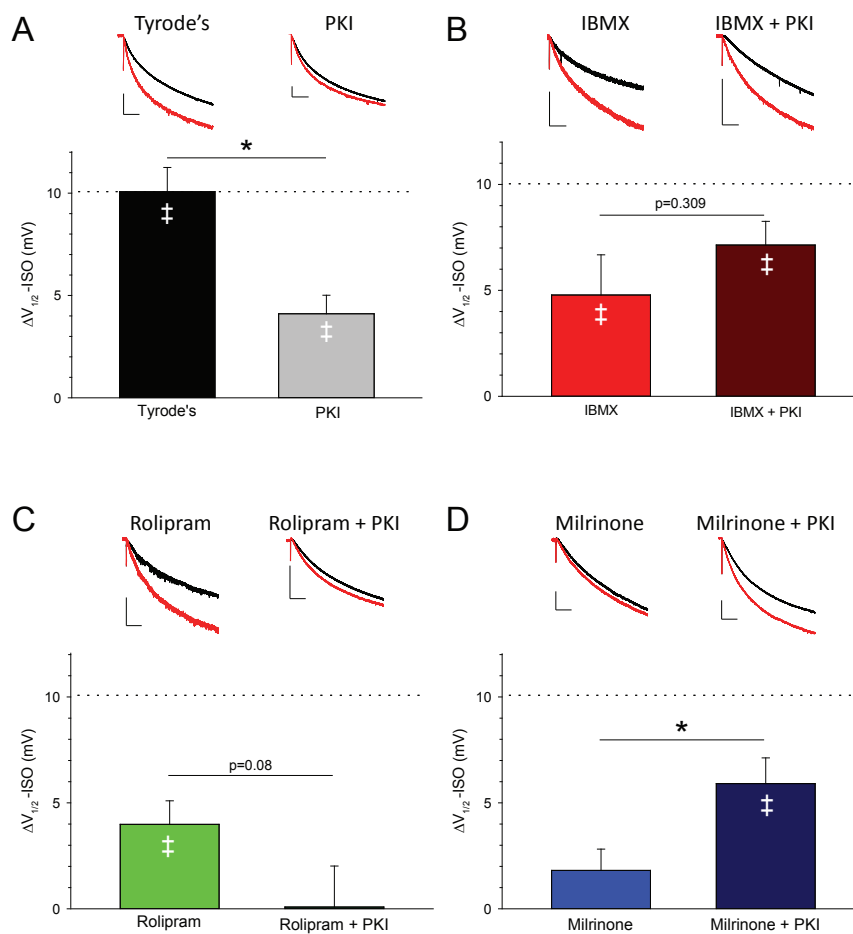


Figure 4. Effects of PDE inhibition on the ability of ISO to shift the voltage-dependence of I_f . The shift in $V_{1/2}$ of I_f in response to ISO ($\Delta V_{1/2}$ -ISO) was determined for individual cells by measuring $V_{1/2}$ values before and after wash-on of ISO in (A) control Tyrode's extracellular solution (black) or Tyrode's solution with PKI (10 μ M) in the patch pipette (grey); (B) IBMX (100 μ M in the extracellular solution; red) or IBMX with PKI in the pipette (dark red); (C) rolipram (10 μ M in the extracellular solution; light green) or rolipram with PKI in the pipette (dark green); and (D) milrinone (50 μ M; blue) or milrinone with PKI in the pipette (dark blue). Dashed lines indicate the $\Delta V_{1/2}$ -ISO shift in control conditions for comparison. Asterisks indicate $p < 0.05$ compared to the corresponding condition without PKI; t -tests. Double daggers indicate a significant shift in response to ISO ($p < 0.05$ versus a hypothetical shift of 0 mV; one-sample t -tests). Insets represent the hyperpolarization-activated currents elicited by single voltage steps to near the midpoint activation voltage for each condition from individual cells before (black) and after (red) wash-on of ISO in the absence (left) or presence (right) of PKI. Scale bars: Tyrode's, 200 pA; PKI, 200 pA; IBMX, 50 pA; IBMX + PKI, 100 pA; rolipram, 100 pA; rolipram + PKI, 200 pA; milrinone, 100 pA; milrinone + PKI, 200 pA. All time scale bars, 500 ms.

4. Discussion

In this study we examined the role of phosphodiesterases in cAMP-dependent regulation of I_f in acutely-isolated sinoatrial node myocytes from mice. We found that the PDE3 and PDE4 isoforms contribute to formation of at least two functional cAMP signaling domains that control I_f in SAMs. The PDE4 family restricts access of cAMP to HCN channels under basal conditions, but does not appear to play a role in the formation of the PKA-dependent β AR-to-HCN channel signaling pathway. Meanwhile, the PDE3 family interacts functionally with PKA to regulate I_f at rest and contributes to the formation of the PKA-dependent pathway between β ARs and HCN channels in SAMs.

Our interpretation of the results assumes that the pharmacological agents we used are relatively selective and that the degree of block achieved is fairly complete. While we cannot exclude the possibility of some off-target block, our results using PKI, IBMX, rolipram, and milrinone cannot be explained by isoform cross-reactivity amongst the blockers. For example, although high concentrations of the PDE3 blocker milrinone ($>10 \mu\text{M}$) can also inhibit PDE4, lower concentrations are thought to be specific for PDE3 [33,35,46]. We tested the effects of $10 \mu\text{M}$ milrinone on I_f , and observed a minimal response (Table 1). To ensure that we had reached a maximal effective concentration in mouse SAMs, and to compare our results to other studies [45], we also evaluated the effects of $50 \mu\text{M}$ milrinone. We found no difference in the response of I_f to 10 or $50 \mu\text{M}$ milrinone (Table 1 [11]). Moreover, the effects of milrinone were qualitatively different from the effects of either the general PDE inhibitor, IBMX, or the PDE4 inhibitor, rolipram. Thus, we conclude that (1) PDE3, alone, has minimal effects on I_f (although it interacts functionally with PKA, see below), and (2) the effects of milrinone on I_f in our experiments did not reflect appreciable block of PDE4.

A key finding of our study is that the shifts in the basal $V_{1/2}$ of I_f produced by IBMX or rolipram were similar in the presence and absence of the PKA inhibitory peptide, PKI. The shifts produced by PDE inhibition alone (without PKA inhibition) could reflect combined effects of direct cAMP binding and PKA phosphorylation, whereas those in the presence of PKI presumably result from a direct effect of cAMP alone. We interpret the similar effects in the presence and absence of PKI as an indication that the cAMP liberated upon total PDE inhibition or PDE4 inhibition activates I_f without a requirement for PKA activity. However, this interpretation assumes that PKI blocks a substantial fraction of the PKA activity near HCN channels in SAMs. We feel that this assumption is justified based on our finding that PKI significantly reduced the shift in $V_{1/2}$ in response to ISO under the same conditions (Figure 4A; Table 1; [11]). A more direct assessment of PKA activity (e.g., PKA assays in sinoatrial node homogenates) would be difficult to interpret because data from tissue extracts is a poor proxy for PKA activity within temporally- and spatially-restricted cAMP signaling domains in SAMs.

The results of the present study extend our previous observations that, although PKA activity is required for βAR signaling to HCN channels in SAMs [11], it is still possible for cAMP to activate I_f in SAMs even in the absence of PKA activity [19]. Taken together, the previous and new data suggest a working model in which members of the PDE4 family form a functional “barrier” that isolates HCN channels from the high basal cAMP in SAMs. Disruption of this barrier with either rolipram or IBMX permits cAMP to access HCN channels, where it activates them via a PKA-independent mechanism (presumably via direct binding to the cyclic nucleotide binding domain of the channels). In our model, PDE3 family members are proposed to form a distinct functional barrier that prevents the cAMP generated upon βAR stimulation from reaching HCN channels directly, thereby constraining βAR signaling to HCN channels to a PKA-dependent pathway. Additional work will be required to determine whether these barriers represent distinct cAMP compartments in SAMs and whether the PKA-dependent activation of I_f by βAR stimulation results from phosphorylation of HCN channels by PKA, or if it occurs as a result of an indirect mechanism, such as control of cAMP production—e.g., by Ca^{2+} -activated adenylyl cyclases [47]—with the resulting cAMP then potentiating I_f by binding directly to HCN channels.

Our observations of differing effects when PDE3 and PKA were inhibited together, instead of individually, indicates a complex functional interaction between PDE3 and PKA in the regulation of I_f in SAMs. The data preclude a simple model in which PDE3 simply acts to restrict the cAMP source that controls PKA regulation of I_f . Instead, there must be co-regulation between PDE3 and PKA. Possible nodes of cross-talk between PDE3 and PKA include the activation of PDE3 by PKA and the inhibition of PDE3 hydrolysis of cAMP by cGMP [35,36]. In the first scenario, inhibition of PKA with PKI would also inhibit PDE3, thereby increasing cAMP, and allowing it to act by binding directly to HCN channels. Consistent with this notion, we found that milrinone, alone, had no significant effect on the $V_{1/2}$ of I_f , but produced a significant depolarizing shift when it was applied in the presence of PKI (Figure 3, Table 1). Meanwhile, a role for cGMP is suggested by the observation of high levels of

soluble guanylyl cyclase and cGMP in the sinoatrial node [48]. Indeed, cGMP-mediated inhibition of PDE3 has been suggested to increase cAMP concentration and accelerate AP firing rate in mouse sinoatrial nodes [49]. cGMP-mediated inhibition of PDE3 has also been shown to modulate cAMP levels in subcellular compartments involved in β AR signaling in ventricular myocytes [50].

Our data complement results of previous studies in which PDEs have been shown to regulate pacemaker activity of the sinoatrial node. Our observations of depolarizing shifts in the voltage dependence of I_f in response to PDE inhibition are in agreement with the notions that the resting cAMP concentration is relatively high in SAMs and that it is limited by constitutive PDE activity [5,33,45,47]. The role of PDE4 in limiting the basal cAMP concentration in the vicinity of HCN channels in our study is in agreement with the observations of Hua et al. [33], who found that inhibition of PDE4 with rolipram (10 μ M) increased AP firing rate and $I_{Ca,L}$ in isolated mouse SAMs to a greater extent than did PDE3 inhibition with milrinone (10 μ M). Our data suggest that I_f works along with $I_{Ca,L}$ to mediate the increase in AP firing rate in response to PDE4 inhibition. Galindo-Tovar and Kaumann [34] used rolipram (1 μ M) along with the PDE3 inhibitor cilostamide (300 nM) to show that both PDE3 and PDE4 contribute to control of basal firing rate in isolated mouse right atria via actions on a cAMP compartment that is distinct from that mediated by β ARs. These data are in good agreement with our observations of multiple functional cAMP signaling domains formed by PDEs in SAMs and of PDE4-dependent regulation of I_f under basal conditions. However, they also suggest that additional PDE3-dependent mechanisms may also contribute to pacemaker activity in the mouse sinoatrial node. Interestingly, β AR-induced tachycardia across many species is resistant to PDE inhibition, suggesting that cAMP signaling between β ARs and relevant effectors for the fight-or-flight increase in heart rate is not controlled by PDEs [51,52]. Hence, β AR regulation of I_f appears to serve primarily as a frequency adaptation mechanism rather than a primary driver of the sympathetic heart rate response. Vinogradova et al. [45] used milrinone (50 μ M) to suggest that PDE3 may be the dominant isoform controlling basal firing rate in rabbit SAMs. However, we did not observe a difference between 10 μ M and 50 μ M milrinone in mouse SAMs, and saw effects of milrinone only in combination with PKA inhibition. Taken together, these data suggest that there may be species-dependent differences in the roles of different PDE isoforms in regulation of sinoatrial node activity.

5. Conclusions

In summary, our results indicate that the PDE3 and PDE4 isoforms create functionally-distinct cAMP signaling domains in mouse SAMs that regulate I_f at rest and in response to β AR stimulation. Specifically, the PDE4 family restricts access of cAMP to HCN4 channels under basal conditions, and the PDE3 family contributes to the formation of a preferred PKA-dependent pathway between β ARs and HCN channels. Given that I_f is a critical factor in sinoatrial node pacemaker activity, it is likely that these mechanisms contribute to the regulation of heart rate.

Acknowledgments: We thank Hicham Bichraoui and Christian Rickert for helpful discussions and critical reading of the manuscript. This work was supported by a grant from the National Heart Lung and Blood Institute (R01-HL088427) to C.P. EJS was supported by 5T32-AG000279 from the National Institute on Aging and F31-HL132408 from the National Heart Lung and Blood Institute. The content is solely the responsibility of the authors and does not necessarily represent the official views of the National Institutes of Health.

Author Contributions: J.R.S. and C.P. designed the experiments. J.R.S., Z.L., E.D.L., E.J.S., and C.P. performed and analyzed the experiments and wrote the manuscript. All authors approved the final version of the manuscript and are accountable for all aspects of the work. All persons designated as authors, and all those who qualify for authorship, are listed.

Conflicts of Interest: The founding sponsors had no role in the design of the study; in the collection, analyses, or interpretation of data; in the writing of the manuscript, and in the decision to publish the results.

Abbreviations

AP	action potential
β AR	adrenergic receptor
cAMP	3',5'-cyclic adenosine monophosphate
HCN channel	hyperpolarization-activated, cyclic nucleotide-sensitive ion channel
IBMX	3-isobutyl-1-methylxanthine
I_f	funny current
ISO	isoproterenol
milr	milrinone
PDE	phosphodiesterase
PKA	cAMP-dependent protein kinase
PKI	PKA inhibitory peptide
roli	rolipram
SAM	sinoatrial node myocyte
$V_{1/2}$	midpoint activation voltage

References

- Mangoni, M.; Nargeot, J. Genesis and regulation of the heart automaticity. *Physiol. Rev.* **2008**, *88*, 919–982. [[CrossRef](#)] [[PubMed](#)]
- Lakatta, E.G.; DiFrancesco, D. What keeps us ticking: A funny current, a calcium clock, or both? *J. Mol. Cell. Cardiol.* **2009**, *47*, 157–170. [[CrossRef](#)] [[PubMed](#)]
- DiFrancesco, D. The role of the funny current in pacemaker activity. *Circ. Res.* **2010**, *106*, 434–446. [[CrossRef](#)] [[PubMed](#)]
- Lakatta, E.G.; Maltsev, V.A.; Vinogradova, T.M. A coupled SYSTEM of intracellular Ca^{2+} clocks and surface membrane voltage clocks controls the timekeeping mechanism of the heart's pacemaker. *Circ. Res.* **2010**, *106*, 659–673. [[CrossRef](#)] [[PubMed](#)]
- Vinogradova, T.; Lyashkov, A.; Zhu, W.; Ruknudin, A.; Sirenko, S.; Yang, D.; Deo, S.; Barlow, M.; Johnson, S.; Caffrey, J.; et al. High basal protein kinase A-dependent phosphorylation drives rhythmic internal Ca^{2+} store oscillations and spontaneous beating of cardiac pacemaker cells. *Circ. Res.* **2006**, *98*, 505–514. [[CrossRef](#)] [[PubMed](#)]
- Liu, J.; Dobrzynski, H.; Yanni, J.; Boyett, M.R.; Lei, M. Organisation of the mouse sinoatrial node: Structure and expression of HCN channels. *Cardiovasc. Res.* **2007**, *73*, 729–738. [[CrossRef](#)] [[PubMed](#)]
- Marionneau, C.; Couette, B.; Liu, J.; Li, H.; Mangoni, M.E.; Nargeot, J.; Lei, M.; Escande, D.; Demolombe, S. Specific pattern of ionic channel gene expression associated with pacemaker activity in the mouse heart. *J. Physiol.* **2005**, *562*, 223–234. [[CrossRef](#)] [[PubMed](#)]
- Moosmang, S.; Stieber, J.; Zong, X.; Biel, M.; Hofmann, F.; Ludwig, A. Cellular expression and functional characterization of four hyperpolarization-activated pacemaker channels in cardiac and neuronal tissues. *Eur. J. Biochem.* **2001**, *268*, 1646–1652. [[CrossRef](#)] [[PubMed](#)]
- Shi, W.; Wymore, R.; Yu, H.; Wu, J.; Wymore, R.T.; Pan, Z.; Robinson, R.B.; Dixon, J.E.; McKinnon, D.; Cohen, I.S. Distribution and Prevalence of Hyperpolarization-Activated Cation Channel (HCN) mRNA Expression in Cardiac Tissues. *Circ. Res.* **1999**, *85*, e1–e6. [[CrossRef](#)] [[PubMed](#)]
- Mangoni, M.E.; Nargeot, J. Properties of the hyperpolarization-activated current (I_f) in isolated mouse sino-atrial cells. *Cardiovasc. Res.* **2001**, *52*, 51–64. [[CrossRef](#)]
- Liao, Z.; Lockhead, D.; Larson, E.; Proenza, C. Phosphorylation and modulation of hyperpolarization-activated HCN4 channels by protein kinase A in the mouse sinoatrial node. *J. Gen. Physiol.* **2010**, *136*, 247–258. [[CrossRef](#)] [[PubMed](#)]
- Verkerk, A.O.; Wilders, R. Pacemaker activity of the human sinoatrial node: An update on the effects of mutations in HCN4 on the hyperpolarization-activated current. *Int. J. Mol. Sci.* **2015**, *16*, 3071–3094. [[CrossRef](#)] [[PubMed](#)]
- Baruscotti, M.; Bucchi, A.; Milanesi, R.; Paina, M.; Barbuti, A.; Gnecci-Ruscione, T.; Bianco, E.; Vitali-Serdoz, L.; Cappato, R.; DiFrancesco, D. A gain-of-function mutation in the cardiac pacemaker HCN4 channel increasing cAMP sensitivity is associated with familial Inappropriate Sinus Tachycardia. *Eur. Heart J.* **2017**, *38*, 280–288. [[CrossRef](#)] [[PubMed](#)]

14. Herrmann, S.; Hofmann, F.; Stieber, J.; Ludwig, A. HCN channels in the heart: Lessons from mouse mutants. *Br. J. Pharmacol.* **2012**, *166*, 501–509. [[CrossRef](#)] [[PubMed](#)]
15. Borer, J.S. Drug insight: If inhibitors as specific heart-rate-reducing agents. *Nat. Clin. Pract. Cardiovasc. Med.* **2004**, *1*, 103–109. [[CrossRef](#)] [[PubMed](#)]
16. Roubille, F.; Tardif, J.-C. New Therapeutic Targets in Cardiology Heart Failure and Arrhythmia: HCN Channels. *Circulation* **2013**, *127*, 1986–1996. [[CrossRef](#)] [[PubMed](#)]
17. DiFrancesco, D.; Tortora, P. Direct activation of cardiac pacemaker channels by intracellular cyclic AMP. *Nature* **1991**, *351*, 145–147. [[CrossRef](#)] [[PubMed](#)]
18. Zagotta, W.N.; Olivier, N.B.; Black, K.D.; Young, E.C.; Olson, R.; Gouaux, E. Structural basis for modulation and agonist specificity of HCN pacemaker channels. *Nature* **2003**, *425*, 200–205. [[CrossRef](#)] [[PubMed](#)]
19. St. Clair, J.R.; Liao, Z.; Larson, E.D.; Proenza, C. PKA-independent activation of I(f) by cAMP in mouse sinoatrial myocytes. *Channels* **2013**, *7*, 318–321.
20. Conti, M.; Mika, D.; Richter, W. Cyclic AMP compartments and signaling specificity: Role of cyclic nucleotide phosphodiesterases. *J. Gen. Physiol.* **2014**, *143*, 29–38. [[CrossRef](#)] [[PubMed](#)]
21. Dodge-Kafka, K.L.; Langeberg, L.; Scott, J.D. Compartmentation of Cyclic Nucleotide Signaling in the Heart the Role of A-Kinase Anchoring Proteins. *Circ. Res.* **2006**, *98*, 993–1001. [[CrossRef](#)] [[PubMed](#)]
22. Karpen, J.W. Perspectives on: Cyclic nucleotide microdomains and signaling specificity. *J. Gen. Physiol.* **2014**, *143*, 5–7. [[CrossRef](#)] [[PubMed](#)]
23. Perera, R.K.; Nikolaev, V.O. Compartmentation of cAMP signalling in cardiomyocytes in health and disease. *Acta Physiol.* **2013**, *207*, 650–662. [[CrossRef](#)] [[PubMed](#)]
24. Richards, M.; Lomas, O.; Jalink, K.; Ford, K.L.; Vaughan-Jones, R.D.; Lefkimiatis, K.; Swietach, P. Intracellular tortuosity underlies slow cAMP diffusion in adult ventricular myocytes. *Cardiovasc. Res.* **2016**, *110*, 395–407. [[CrossRef](#)] [[PubMed](#)]
25. Warriar, S.; Ramamurthy, G.; Eckert, R.L.; Nikolaev, V.O.; Lohse, M.J.; Harvey, R.D. cAMP microdomains and L-type Ca²⁺ channel regulation in guinea-pig ventricular myocytes. *J. Physiol.* **2007**, *580*, 765–776. [[CrossRef](#)] [[PubMed](#)]
26. Xiang, Y. Compartmentalization of beta-adrenergic signals in cardiomyocytes. *Circ. Res.* **2011**, *109*, 231–244. [[CrossRef](#)] [[PubMed](#)]
27. Zaccolo, M. cAMP signal transduction in the heart: Understanding spatial control for the development of novel therapeutic strategies. *Br. J. Pharmacol.* **2009**, *158*, 50–60. [[CrossRef](#)] [[PubMed](#)]
28. Jurevicius, J.; Fischmeister, R. cAMP compartmentation is responsible for a local activation of cardiac Ca²⁺ channels by beta-adrenergic agonists. *Proc. Natl. Acad. Sci. USA* **1996**, *93*, 295–299. [[CrossRef](#)] [[PubMed](#)]
29. Steinberg, S.F.; Brunton, L.L. Compartmentation of G Protein-Coupled Signaling Pathways in Cardiac Myocytes. *Annu. Rev. Pharmacol. Toxicol.* **2001**, *41*, 751–773. [[CrossRef](#)] [[PubMed](#)]
30. Zaccolo, M.; Pozzan, T. Discrete microdomains with high concentration of cAMP in stimulated rat neonatal cardiac myocytes. *Science* **2002**, *295*, 1711–1715. [[CrossRef](#)] [[PubMed](#)]
31. Jurevicius, J.; Skeberdis, V.A.; Fischmeister, R. Role of cyclic nucleotide phosphodiesterase isoforms in cAMP compartmentation following beta2-adrenergic stimulation of I_{Ca,L} in frog ventricular myocytes. *J. Physiol.* **2003**, *551*, 239–252. [[CrossRef](#)] [[PubMed](#)]
32. Mongillo, M.; McSorley, T.; Evellin, S.; Sood, A.; Lissandron, V.; Terrin, A.; Huston, E.; Hannawacker, A.; Lohse, M.J.; Pozzan, T.; et al. Fluorescence Resonance Energy Transfer-Based Analysis of cAMP Dynamics in Live Neonatal Rat Cardiac Myocytes Reveals Distinct Functions of Compartmentalized Phosphodiesterases. *Circ. Res.* **2004**, *95*, 67–75. [[CrossRef](#)] [[PubMed](#)]
33. Hua, R.; Adamczyk, A.; Robbins, C.; Ray, G.; Rose, R. Distinct patterns of constitutive phosphodiesterase activity in mouse sinoatrial node and atrial myocardium. *PLoS ONE* **2012**, *7*, e47652. [[CrossRef](#)] [[PubMed](#)]
34. Galindo-Tovar, A.; Kaumann, A.J. Phosphodiesterase-4 blunts inotropism and arrhythmias but not sinoatrial tachycardia of (–)-adrenaline mediated through mouse cardiac β1-adrenoceptors. *Br. J. Pharmacol.* **2008**, *153*, 710–720. [[CrossRef](#)] [[PubMed](#)]
35. Shakur, Y.; Fong, M.; Hensley, J.; Cone, J.; Movsesian, M.; Kambayashi, J.; Yoshitake, M.; Liu, Y. Comparison of the effects of cilostazol and milrinone on cAMP-PDE activity, intracellular cAMP and calcium in the heart. *Cardiovasc. Drugs Ther. Spons. Int. Soc. Cardiovasc. Pharmacother.* **2002**, *16*, 417–427. [[CrossRef](#)]
36. Zaccolo, M.; Movsesian, M. cAMP and cGMP signaling cross-talk: Role of phosphodiesterases and implications for cardiac pathophysiology. *Circ. Res.* **2007**, *100*, 1569–1578. [[CrossRef](#)] [[PubMed](#)]

37. Liao, Z.; St. Clair, J.R.; Larson, E.D.; Proenza, C. Myristoylated peptides potentiate the funny current (I_f) in sinoatrial myocytes. *Channels* **2011**, *5*, 115–119. [[CrossRef](#)] [[PubMed](#)]
38. Groenke, S.; Larson, E.D.; Alber, S.; Zhang, R.; Lamp, S.T.; Ren, X.; Nakano, H.; Jordan, M.C.; Karagueuzian, H.S.; Roos, K.P.; et al. Complete atrial-specific knockout of sodium-calcium exchange eliminates sinoatrial node pacemaker activity. *PLoS ONE* **2013**, *8*, e81633. [[CrossRef](#)] [[PubMed](#)]
39. St. Clair, J.R.; Sharpe, E.J.; Proenza, C. Culture and adenoviral infection of sinoatrial node myocytes from adult mice. *Am. J. Physiol. Heart Circ. Physiol.* **2015**, *309*, H490–H498. [[CrossRef](#)] [[PubMed](#)]
40. Larson, E.D.; St. Clair, J.R.; Sumner, W.A.; Bannister, R.A.; Proenza, C. Depressed pacemaker activity of sinoatrial node myocytes contributes to the age-dependent decline in maximum heart rate. *Proc. Natl. Acad. Sci. USA* **2013**, *110*, 18011–18016. [[CrossRef](#)] [[PubMed](#)]
41. Sharpe, E.J.; St. Clair, J.R.; Proenza, C. Methods for the Isolation, Culture, and Functional Characterization of Sinoatrial Node Myocytes from Adult Mice. *J. Vis. Exp.* **2016**. [[CrossRef](#)] [[PubMed](#)]
42. Sharpe, E.J.; Larson, E.D.; Proenza, C. Cyclic AMP reverses the effects of aging on pacemaker activity and I_f in sinoatrial node myocytes. *J. Gen. Physiol.* **2017**, *149*, 237–247. [[CrossRef](#)] [[PubMed](#)]
43. Barry, P.H. JPCalc, a software package for calculating liquid junction potential corrections in patch-clamp, intracellular, epithelial and bilayer measurements and for correcting junction potential measurements. *J. Neurosci. Methods* **1994**, *51*, 107–116. [[CrossRef](#)]
44. Kaumann, A.J.; Galindo-Tovar, A.; Escudero, E.; Vargas, M.L. Phosphodiesterases do not limit beta1-adrenoceptor-mediated sinoatrial tachycardia: Evidence with PDE3 and PDE4 in rabbits and PDE1–5 in rats. *Naunyn. Schmiedebergs Arch. Pharmacol.* **2009**, *380*, 421–430. [[CrossRef](#)] [[PubMed](#)]
45. Vinogradova, T.; Sirenko, S.; Lyashkov, A.; Younes, A.; Li, Y.; Zhu, W.; Yang, D.; Ruknudin, A.; Spurgeon, H.; Lakatta, E. Constitutive phosphodiesterase activity restricts spontaneous beating rate of cardiac pacemaker cells by suppressing local Ca²⁺ releases. *Circ. Res.* **2008**, *102*, 761–769. [[CrossRef](#)] [[PubMed](#)]
46. Kerfant, B.-G.; Zhao, D.; Lorenzen-Schmidt, I.; Wilson, L.S.; Cai, S.; Chen, S.R.W.; Maurice, D.H.; Backx, P.H. PI3Kγ Is Required for PDE4, not PDE3, Activity in Subcellular Microdomains Containing the Sarcoplasmic Reticular Calcium ATPase in Cardiomyocytes. *Circ. Res.* **2007**, *101*, 400–408. [[CrossRef](#)] [[PubMed](#)]
47. Mattick, P.; Parrington, J.; Oda, E.; Simpson, A.; Collins, T.; Terrar, D. Ca²⁺-stimulated adenylyl cyclase isoform AC1 is preferentially expressed in guinea-pig sino-atrial node cells and modulates the I_f pacemaker current. *J. Physiol.* **2007**, *582*, 1195–1203. [[CrossRef](#)] [[PubMed](#)]
48. Brahmajothi, M.V.; Campbell, D.L. Heterogeneous expression of NO-activated soluble guanylyl cyclase in mammalian heart: Implications for NO- and redox-mediated indirect versus direct regulation of cardiac ion channel function. *Channels* **2007**, *1*, 353–365. [[CrossRef](#)] [[PubMed](#)]
49. Abramochkin, D.V.; Konovalova, O.P.; Kamkin, A.; Sitdikova, G.F. Carbon monoxide modulates electrical activity of murine myocardium via cGMP-dependent mechanisms. *J. Physiol. Biochem.* **2015**, *71*, 107–119. [[CrossRef](#)] [[PubMed](#)]
50. Stangherlin, A.; Gesellchen, F.; Zoccarato, A.; Terrin, A.; Fields, L.A.; Berrera, M.; Surdo, N.C.; Craig, M.A.; Smith, G.; Hamilton, G.; et al. cGMP Signals Modulate cAMP Levels in a Compartment-Specific Manner to Regulate Catecholamine-Dependent Signaling in Cardiac Myocytes. *Circ. Res.* **2011**, *108*, 929–939. [[CrossRef](#)] [[PubMed](#)]
51. Galindo-Tovar, A.; Vargas, M.L.; Kaumann, A.J. Inhibitors of phosphodiesterases PDE2, PDE3, and PDE4 do not increase the sinoatrial tachycardia of noradrenaline and prostaglandin PGE1 in mice. *Naunyn. Schmiedebergs Arch. Pharmacol.* **2016**, *389*, 177–186. [[CrossRef](#)] [[PubMed](#)]
52. Kaumann, A.J. Phosphodiesterases reduce spontaneous sinoatrial beating but not the “fight or flight” tachycardia elicited by agonists through Gs-protein-coupled receptors. *Trends Pharmacol. Sci.* **2011**, *32*, 377–383. [[CrossRef](#)] [[PubMed](#)]

